International Journal of Nanoscience
Vol. 7, No. 6 (2008) 325–331

World Scientific
www.worldscientific.com

CONVECTIVE HEAT TRANSFER CHARACTERISTICS OF AQUEOUS TiO_2 NANOFLUID UNDER LAMINAR FLOW CONDITIONS

S. M. SOHEL MURSHED*, KAI CHOONG LEONG,
CHUN YANG and NAM-TRUNG NGUYEN
School of Mechanical and Aerospace Engineering
Nanyang Technological University
50 Nanyang Avenue, Singapore 639798
**murshedsms@pmail.ntu.edu.sg*

Revised 15 October 2008

This paper reports an experimental investigation into force convective heat transfer of nanofluids flowing through a cylindrical minichannel under laminar flow and constant wall heat flux conditions. Sample nanofluids were prepared by dispersing different volumetric concentrations (0.2–0.8%) of nanoparticles in deionized water. The results showed that both the convective heat transfer coefficient and the Nusselt number of the nanofluid increase considerably with the nanoparticle volume fraction as well as the Reynolds number. Along with the enhanced thermal conductivity of nanofluids, the migration, interactions, and Brownian motion of nanoparticles and the resulting disturbance of the boundary layer are responsible for the observed enhancement of heat transfer coefficients of nanofluids.

Keywords: Nanofluids; nanoparticles; convective heat transfer; microchannel.

1. Introduction

Over the last several decades, scientists and engineers have been attempting to develop fluids which can offer better cooling or heating performance for a variety of thermal systems compared to conventional heat transfer fluids. Applying nanotechnology to thermal engineering, the novel concept of "nanofluids", which was coined at the Argonne National Laboratory of the USA by Stev Choi in 1995, has been proposed as a means of meeting these cooling challenges.[1] This new class of heat transfer fluids is engineered by dispersing nanometer-sized solid particles in traditional heat transfer fluids such as water, ethylene glycol, or engine oil. From the investigations in the past decade, nanofluids were found to exhibit significantly higher thermal properties, particularly effective thermal conductivity[2–8] and effective thermal diffusivity,[9] compared to their base fluids. Aiming at the potential application of nanofluids in advanced cooling techniques for more efficient cooling of electronics and microelectromechanical systems (MEMSs), studies on convective heat transfer of nanofluids are of great interest. However, compared to the reported research efforts on effective thermal conductivity, only a handful were performed for convective heat transfer of nanofluids. Since the concept of nanofluids is relatively new and its heat transfer characteristics are not well understood by the researchers, a short review of reported studies, particularly on

force convection of nanofluids, will be discussed here.

The first experiment on convective heat transfer of nanofluids (e.g. γ-Al_2O_3/water) under turbulent flow conditions was performed by Pak and Cho.[10] In their study, even though the Nusselt number (Nu) was found to increase with the particle volume fraction and the Reynolds number, the heat transfer coefficient (h) actually decreased by 3–12%. On the other hand, Eastman *et al.* later showed that with less than 1 vol% of CuO nanoparticles, the convective heat transfer coefficient of water was increased by more than 15%.[11] The experimental results of Xuan and Li illustrated that the Nusselt number of Cu/water-based nanofluids varied significantly with the flow velocity and the volumetric loading of particles.[12] For example, for 2 vol% of Cu nanoparticles in water, the Nusselt number increased by about 60% and the Dittus–Boelter correlation[13] was unable to predict such an enhanced Nusselt number.

Wen and Ding reported the heat transfer behavior of nanofluids at the tube entrance region under laminar flow conditions.[14] Their results showed that the local heat transfer coefficient varied with the particle volume fraction (ϕ) and the Reynolds number (Re). For the case of $\phi = 0.016$ and dimensionless axial distance $x/D \approx 63$ from the entrance, the local h was 41% higher for Re = 1050, and 47% higher for Re = 1600, compared with the results for pure water. They also observed that the enhancement is particularly significant at the entrance region. The same research group later studied the convective heat transfer of CNT-based nanofluids under laminar flow and constant wall heat flux conditions.[15] Surprisingly, the maximum increase of the local h was more than 350% at Re = 800 and at 0.5 wt% of the carbon nanotube (CNT). Convective heat transfer of CuO and Al_2O_3/water-based nanofluids under laminar flow conditions through an annular tube was investigated by Heris *et al.*[16] Their results showed an enhanced heat transfer coefficient, which increased with an increasing particle volume fraction as well as Peclet number. Results for Al_2O_3/water-based nanofluids showed higher enhancement of the heat transfer coefficient compared to CuO/water-based nanofluids. Recently, Jung *et al.* conducted heat transfer experiments for Al_2O_3/water-based nanofluids in a rectangular microchannel (50 μm × 50 μm) under laminar flow conditions.[17] The convective heat transfer coefficient increased by more than 32% with 1.8 vol% of nanoparticles and the Nusselt number increased with an increasing Reynolds number in the laminar flow regime ($5 > \text{Re} < 300$).

The above review demonstrated that the results reported by various groups vary widely and most of the studies lack physical explanation for their observed results. There is therefore a need for more research efforts on convective heat transfer of nanofluids. In this study, convective heat transfer of nanofluids under laminar flow conditions is presented and the results are analyzed.

2. Experimental Setup and Procedure

An experimental setup was established to conduct experiments on heat transfer of nanofluids in the laminar flow regime in a cylindrical channel. The experimental facility consisted of a flow loop, a heating unit, a cooling system, and a measuring and control unit. The flow loop consisted of a pump, a test section, a flow meter, a dampener, and a reservoir. The measuring and control unit included an HP data logger with bench link data acquisition software and a personal computer. A schematic of the experimental facility is shown in Fig. 1.

In this study, a straight copper tube of 360 mm length, 4 mm inner diameter and 6 mm outer diameter was used as flowing channel. A peristaltic pump from Cole-Parmer International, USA, with a variable speed of 6–600 RPM and a flow rate ranging from 0.36 to 3400 mL/min, was employed to maintain different flow rates for the required Reynolds number. To minimize the vibration and to ensure steady flow, a flow dampener was also used between the pump and the flow meter. An electric microcoil heater (Chong Mei Heater Co. Ltd., Singapore) was used to obtain a constant wall heat flux boundary condition. A voltmeter and an ammeter were connected to the loop to measure the voltage and the current, respectively. The heater (3.5 kW maximum capacity) was connected to the adjustable ac power supply, which had a maximum power of 240 V. In order to minimize the heat loss, the entire test section was thermally insulated. The hydrodynamic entry section was long enough to accomplish fully developed flow at the heat transfer test section. Five K-type thermocouples were mounted on the test section at the axial positions of 100 mm (T_{w1}), 160 mm (T_{w2}), 220 mm (T_{w3}), 280 mm (T_{w4}), and 340 mm (T_{w5}) from the inlet of the test section to measure the wall temperature

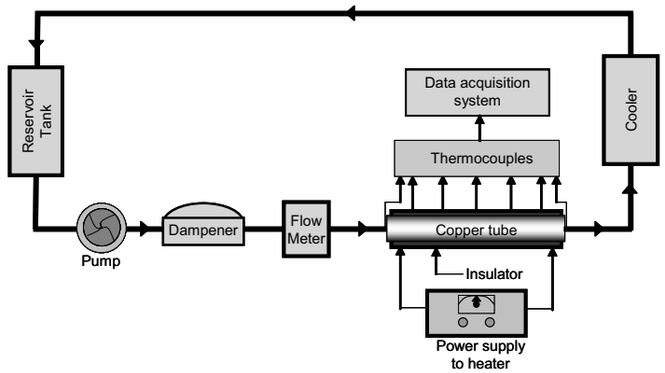

Fig. 1. Schematic of the experimental setup.

distribution. In addition, two thermocouples were mounted at the inlet and exit of the copper tube to measure the bulk temperature of the nanofluids. A tank with running water was used as the cooling system, and test fluid was run through the copper coils before exiting the water tank.

During the experiment, the pump flow rate, voltage, and current of the power supply were recorded and the temperature readings from the thermocouples were registered by the data acquisition system. By making use of these temperature readings and supplied heat flux into appropriate expressions (see the following section), the heat transfer coefficients (h and Nu) were then calculated.

3. Data Processing

The cooling heat transfer performance of nanofluids was defined in terms of the following local convective heat transfer coefficient:

$$h_{\mathrm{nf}-x} = \frac{q''}{T_{i,w}(x) - T_m(x)}\,, \tag{1}$$

where $h_{\mathrm{nf}-x}$ is the local heat transfer coefficient of nanofluids (W/m^2K), $q'' = (\dot{m}c_p(T_{\mathrm{out}} - T_{\mathrm{in}}))/\pi D_i L$ is the heat flux of the heat transfer test section, D_i is the inner diameter of the tube (also the hydrodynamic diameter), $T_{i,w}(x)$ is the inner wall temperature of the tube, L is the length of the test section, $\dot{m}(= \rho u A_c)$ is the mass flow rate (kg/s), c_p is the specific heat of the fluid, and $T_m(x)$ is the mean bulk fluid temperature at the axial position x.

Since the inner wall temperature of the tube, $T_{i,w}(x)$, could not be measured directly for an electrically heated tube, it can be determined from the heat conduction equation in the cylindrical coordinates as given[18]:

$$T_{i,w}(x) = T_{o,w}(x) - \frac{q[2D_o^2 \ln(D_o/D_i) - (D_o^2 - D_i^2)]}{4\pi(D_o^2 - D_i^2)k_s x}\,, \tag{2}$$

where $T_{o,w}(x)$ is the outer wall temperature of the tube (measurable), q is the heat supplied to the test section (W), k_s is the thermal conductivity of the tube, i.e. the copper tube, D_o is the outer diameter of the tube, and x represents the longitudinal location of the section of interest from the entrance.

The mean bulk fluid temperature, $T_m(x)$, at the section of interest can be determined from an energy balance in any section of the tube for a constant surface heat flux condition. From the first law (energy balance) for the control volume of length, dx of the tube with incompressible liquid and for negligible pressure, we can write

$$dq_{\mathrm{conv}} = q'' p dx = \dot{m}c_p dT_m\,, \tag{3}$$

where the perimeter of the cross section $p = \pi D_i$ and dT_m is the differential mean temperature of the fluid in that section.

Rearranging Eq. (3),

$$dT_m = \frac{q''\pi D_i}{\dot{m}c_p} dx\,. \tag{4}$$

The variation of T_m with respect to x is determined by integrating from $x = 0$ to x and, simplifying, we have

$$T_m(x) = T_{\mathrm{in}} + \frac{(T_{\mathrm{out}} - T_{\mathrm{in}})}{L} x\,. \tag{5}$$

Substituting Eqs. (2) and (5) into Eq. (1), the local heat transfer coefficient can be obtained from

$$h_{\mathrm{nf}-x} = \frac{q''}{\left\{T_{o,w}(x) - \dfrac{q[2D_o^2 \ln(D_o/D_i) - (D_o^2 - D_i^2)]}{4\pi(D_o^2 - D_i^2)k_s x}\right\} - \left\{T_{\mathrm{in}} + \dfrac{(T_{\mathrm{out}} - T_{\mathrm{in}})}{L}x\right\}}. \quad (6)$$

By applying the measured wall and fluid temperatures as well as the heat flux into Eq. (6), the local heat transfer coefficient is determined in this study.

Once the local heat transfer coefficient is determined and the thermal conductivity of the medium is known, a local Nusselt number is calculated from

$$Nu_{\mathrm{nf}-x} = \frac{h_{\mathrm{nf}-x} D_i}{k_{\mathrm{nf}}}, \quad (7)$$

where k_{nf} is the effective thermal conductivity of nanofluids. The classical Hamilton–Crosser model is used for the determination of the effective thermal conductivity of nanofluids (k_{nf}), which is given by[19]

$$k_{\mathrm{nf}} = k_f \left[\frac{k_p + (n-1)k_f - (n-1)\phi(k_f - k_p)}{k_p + (n-1)k_f + \phi(k_f - k_p)}\right], \quad (8)$$

where k_f and k_p are the thermal conductivities of the base liquid and the nanoparticles, respectively, ϕ is the volume fraction of nanoparticles, and n is the empirical shape factor, which has a value of 3 for the spherical particle.

The Nusselt number can also be determined from the existing correlations. The well-known Shah correlation for laminar flows under the constant heat flux boundary conditions is given as[20]

$$\mathrm{Nu} = 1.953\left(\mathrm{Re}\,\mathrm{Pr}\frac{D}{x}\right)^{1/3} \quad \text{for} \quad \left(\mathrm{Re}\,\mathrm{Pr}\frac{D}{x}\right) \geq 33.3. \quad (9)$$

For steady and incompressible flow of nanofluids in a tube of uniform cross-sectional area, the Reynolds number and Prandtl number are defined as follows:

$$\mathrm{Re} = \frac{4\dot{m}}{\pi D_i \mu_{\mathrm{nf}}} \quad \text{and} \quad \mathrm{Pr} = \frac{c_{p-\mathrm{nf}}\mu_{\mathrm{nf}}}{k_{\mathrm{nf}}}, \quad (10)$$

where $\dot{m}$ is the mass flow rate and μ_{nf}, $c_{p-\mathrm{nf}}$, and k_{nf} are the viscosity, specific heat, and thermal conductivity of nanofluids, respectively.

While the specific heat of nanofluids is calculated using the volume fraction mixture rule[10]

$$c_{p-\mathrm{nf}} = \phi c_{p-p} + (1-\phi)c_{p-f}, \quad (11)$$

the viscosity of nanofluids is determined from Batchelor's model, given by[21]

$$\mu_{\mathrm{nf}} = \mu_f(1 + 2.5\phi + 6.2\phi^2), \quad (12)$$

where ϕ is the particle volume fraction and μ_f is the base fluid viscosity. It is noted that other classical models for calculating the viscosity of mixture yield similar results.[8]

In this study, experimentally determined Nusselt numbers are compared with the predictions by the Shah correlation [Eq. (9)].

4. Sample Preparation

Since nanofluid is not just a simple mixture of liquid and solid nanoparticles, proper mixing of nanoparticles is very important. The properties and behavior of a suspension depend on the liquid and suspended particle size, as well as the quality of dispersion of the particles in the liquid. Sample nanofluids were prepared by dispersing different vol%, i.e., 0.2–0.8%, of titanium dioxide (TiO_2) nanoparticles (spherical and 15 nm diameter) in deionized water (DIW). To ensure proper dispersion of nanoparticles, the sample nanofluid was homogenized by using an ultrasonic dismembrator (Fisher Scientific Model 500) and a magnetic stirrer. Cetyl trimethyl ammonium bromide (CTAB) surfactant of 0.1 mM concentration was used as a dispersant agent to ensure better dispersion of nanoparticles.

5. Calibration and Uncertainty Analysis

The significant errors that could influence the accuracy of the experimental data can be classified into two groups: systematic errors and random errors. While systematic errors are minimized with careful experimentation and the calibration operations, the precision error can be treated statistically.

Calibration of the thermocouples was done using a calibration bath. Before measuring the heat transfer coefficient of nanofluids, the experimental system was calibrated with DIW.

The experimental uncertainties are estimated by the guidelines described in Ref. 22. The

uncertainty for the measurements of the heat transfer coefficient and Nusselt number can be estimated from the following equations, respectively:

$$\frac{\delta h}{h} = \sqrt{\left(\frac{\delta T}{T}\right)^2 + \left(\frac{\delta q''}{q''}\right)^2 + \left(\frac{\delta \dot{m}}{\dot{m}}\right)^2}, \quad (13a)$$

$$\frac{\delta \mathrm{Nu}}{\mathrm{Nu}} = \sqrt{\begin{array}{c}\left(\frac{\delta T}{T}\right)^2 + \left(\frac{\delta q''}{q''}\right)^2 + \left(\frac{\delta \dot{m}}{\dot{m}}\right)^2 \\ + \left(\frac{\delta D}{D}\right)^2 + \left(\frac{\delta k}{k}\right)^2.\end{array}} \quad (13b)$$

The thermocouples were calibrated and their accuracy of temperature readings was within ± 0.5 K. The accuracy of the heat flux generated by a heater connected to the power source was less than 2%. The pump performance was calibrated by a simple timed weighting method. The accuracy of the flow rate measured by a flow meter was within 0.2%. The accuracy of the tube diameter (D) was less than 0.1%. Since the effective thermal conductivity of nanofluids was calculated from the classical Hamilton–Crosser model, its uncertainty was ignored.

From Eqs. (13) the uncertainty of the measured heat transfer coefficient (h) and Nusselt number (Nu) were estimated to be $\pm 2.1\%$ and $\pm 2.2\%$, respectively.

6. Results and Discussion

The effects of axial position, nanoparticle concentration, and Reynolds number on the heat transfer characteristics of TiO_2/DIW-based nanofluids are investigated and the results are discussed. The range of Reynolds numbers was 900–1700.

6.1. *Axial profiles of the convective heat transfer coefficient*

Figures 2(a) and 2(b) illustrate the local heat transfer coefficient against the axial distance from the entrance of the test section at two Reynolds numbers, Re = 1100 and Re = 1700. The results show that nanofluids exhibit a considerably enhanced convective heat transfer coefficient, which also increases with volumetric loading of nanoparticles. For example, at 0.8 vol% of nanoparticles and at position $x/D = 25$, the local heat transfer coefficient of this nanofluid was found to be about 12% and 14% higher compared to DIW at Re = 1100 and 1700, respectively (Fig. 2). These enhanced heat transfer coefficients of nanofluids is because of the enhanced effective thermal conductivity and the acceleration of the energy exchange process in the fluid due to the random movements of the nanoparticles. Another reason for such enhancement can be the migration of nanoparticles in base fluids due to the shear action, viscosity gradient, and Brownian motion in the cross section of the tube.[14]

Figure 3 depicts the comparison of results obtained from the Shah correlation [Eq. (9)] and measured Nusselt numbers along the axial distance. The Shah correlation slightly overpredicts the present results. The difference in tube size may be one of the reasons for such overprediction. A relatively small tube (4 mm diameter) was used in this experiment, whereas the Shah equation was developed on the basis of laminar flow in large channels.

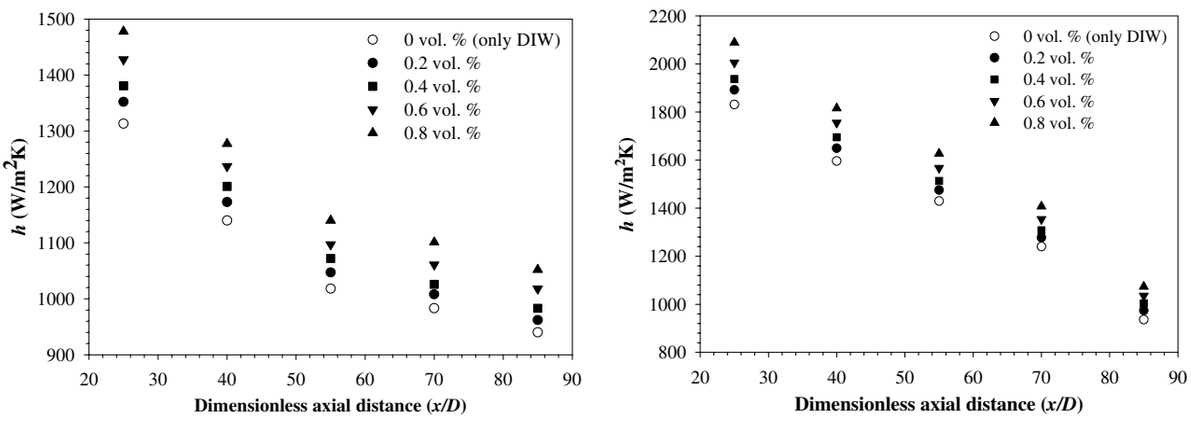

Fig. 2. Axial profiles of the local heat transfer coefficient: (a) Re = 1100 and (b) Re = 1700.

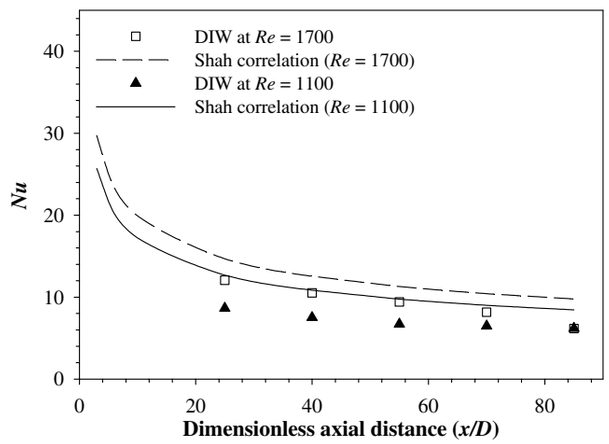

Fig. 3. Comparison with the Shah correlation along the axial distance at Re = 1100 and 1700.

Nevertheless, similar overprediction by the Shah equation was also reported by Wen and Ding.[14]

6.2. *Effect of the Reynolds number on the Nusselt number*

The effect of the Reynolds number on the Nusselt number is shown in Fig. 4. It is seen that the measured Nusselt numbers for nanofluids are higher than those for water and they increase remarkably with the Reynolds number. The observed enhancement of the Nusselt number could be due to the suppression of the boundary layer, the viscosity of nanofluids, as well as dispersion of the nanoparticles.

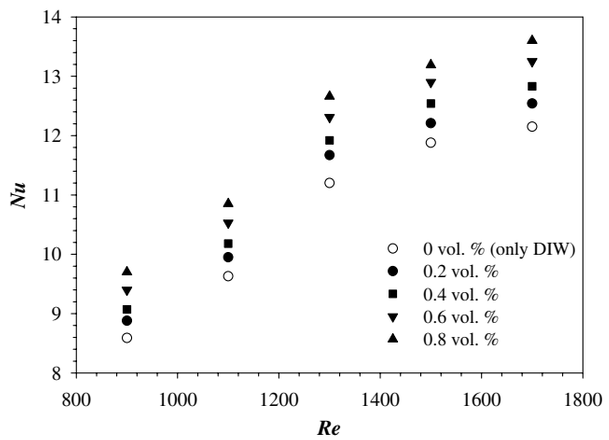

Fig. 4. Reynolds number versus Nusselt number at location $x/D = 25$.

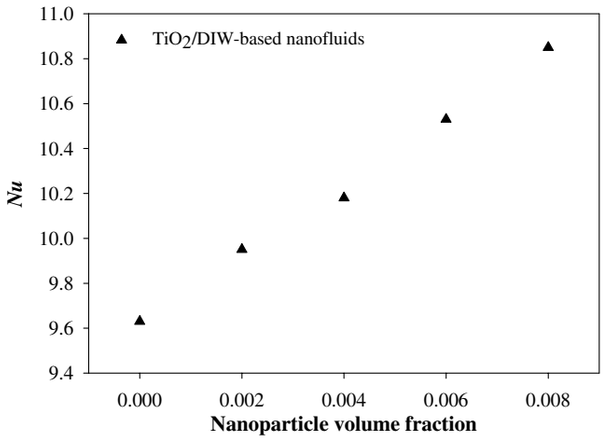

Fig. 5. Particle volume fraction versus Nusselt number at $x/D = 25$ and Re = 1100.

6.3. *Effect of nanoparticle concentration on the Nusselt number*

Figure 5 demonstrates particle volume fraction dependence of the Nusselt number. As can be seen, the Nusselt number of nanofluids increases almost linearly with the particle volume fraction. The nanofluid behaves more like a fluid than a conventional solid–fluid mixture in which larger particles (micrometer or millimeter) are suspended. The effects of several factors, such as gravity, Brownian force, and friction force between the fluid and the ultrafine particles, may coexist in the main flow of nanofluids.

7. Conclusions

An experimental study on force convective heat transfer of a nanofluid flowing through a minichannel under laminar flow conditions has been presented. The results show that nanofluid exhibits an enhanced heat transfer coefficient compared to its base fluid. Both the heat transfer coefficient and the Nusselt number increase significantly with the nanoparticle volume fraction and Reynolds number. Along with the enhanced effective thermal conductivity and viscosity of nanofluids, the migration and random movement of nanoparticles and the resulting disturbance of the boundary layer are the reasons for such increase in convective heat transfer coefficients of nanofluids. Further investigations are needed for a better understanding of the underlying mechanisms for enhanced heat transfer characteristics of nanofluids.

References

1. S. U. S. Choi, in *Developments and Applications of non-Newtonian Flows*, eds. D. A. Siginer and H. P. Wang, *FED*, Vol. 231/*MD*, Vol. 66 (ASME, New York, 1995).
2. J. A. Eastman, S. U. S. Choi, S. Li and L. J. Thompson, in *Proc. Symp. Nanophase and Nanocomposite Materials II* (Materials Research Society, USA, 457, 1997), pp. 3–11.
3. S. Lee, S. U. S. Choi, S. Li and J. A. Eastman, *J. Heat Transfer* **121**, 280 (1999).
4. S. K. Das, N. Putra, P. Thiesen and W. Roetzel, *J. Heat Transfer* **125**, 567 (2003).
5. S. M. S. Murshed, K. C. Leong and C. Yang, *Int. J. Therm. Sci.* **44**, 367 (2005).
6. C. H. Li and G. P. Peterson, *J. Appl. Phys.* **99**, 084314 (2006).
7. S. M. S. Murshed, K. C. Leong and C. Yang, *Int. J. Nanosci.* **5**, 23 (2006).
8. S. M. S. Murshed, K. C. Leong and C. Yang, *Int. J. Therm. Sci.* **47**, 560 (2008).
9. S. M. S. Murshed, K. C. Leong and C. Yang, *J. Phys. D* **39**, 5316 (2006).
10. B. C. Pak and Y. I. Cho, *Exp. Heat Transfer* **11**, 151 (1998).
11. J. A. Eastman, S. U. S. Choi, S. Li, G. Soyez, L. J. Thompson and R. J. Dimelfi, *Mater. Sci. Forum* **312–314**, 629 (1999).
12. Y. Xuan and Q. Li, *J. Heat Transfer* **125**, 151 (2003).
13. F. W. Dittus and L. M. K. Boelter, *University of California Publications on Engineering, Berkeley* **2**, 443 (1930).
14. D. Wen and Y. Ding, *Int. J. Heat Mass Transfer* **47**, 5181 (2004).
15. Y. Ding, H. Alias, D. Wen and A. R. Williams, *Int. J. Heat Mass Transfer* **49**, 240 (2006).
16. S. Z. Heris, S. G. Etemad and M. S. Esfahany, *Int. Comm. Heat Mass Transfer* **33**, 529 (2006).
17. J.-Y. Jung, H.-S. Oh and H.-Y. Kwak, in *Proc. ASME Int. Mech. Eng. Cong. Expos.* (USA, 2006).
18. B. C. Pak, Y. I. Cho and S. U. S. Choi, *Int. J. Heat Mass Transfer* **34**, 1195 (1991).
19. R. L. Hamilton and O. K. Crosser, *Ind. Eng. Chem. Fund.* **1**, 187 (1962).
20. A. Bejan, *Convection Heat Transfer*, 3rd edn. (John Wily & Sons, New York, 2004).
21. G. K. Batchelor, *J. Fluid Mech.* **83**, 97 (1977).
22. R. J. Moffat, *J. Fluid Eng.* **107**, 173 (1985).

February 10, 2009 18:38 00549